Electronic Supplementary Material (ESI) for Physical Chemistry Chemical Physics.

Supporting Information

Fast magnesium ion conducting isopropylamine magnesium borohydride enhanced by hydrophobic interactions

Lasse G. Kristensen,[1] Mads B. Amdisen,[1] Lasse N. Skov,[1] and Torben R. Jensen[1*]

[1] *Interdisciplinary Nanoscience Center (iNANO) and Department of Chemistry, University of Aarhus, Langelandsgade 140, DK-8000 Aarhus C, Denmark.*

** Corresponding author T. R. Jensen, E-mail: trj@chem.au.dk, orcid: 0000-0002-4278-322.*

Electrochemical impedance spectroscopy (SI1)

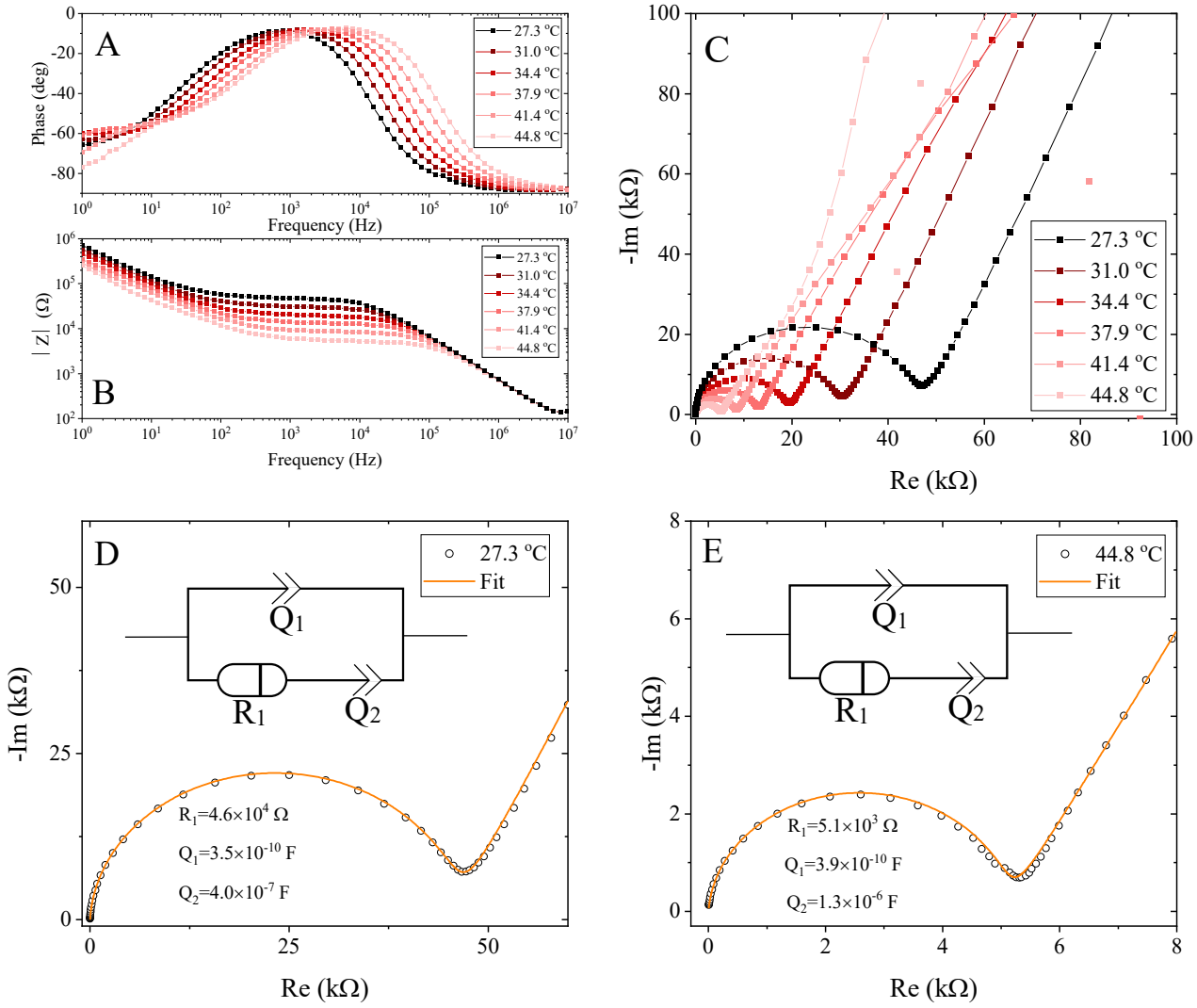

*Figure S1. Bode plot (A and B) and Nyquist plot (C) of $Mg(BH_4)_2$·1.5-IPA (**s5***) from 1 Hz to 1×10^7 Hz at 28 °C to 45 °C. (D) and (E) are EIS data and fits to the equivalent circuit seen in both figures C and D at 27 °C and 45 °C. *Measurements were done on a new batch to reproduce the results reported in the article. However, due to a slightly different composition conductivity is lowered by a factor 2.*

In Figure S1 Bode and Nyquist plots of $Mg(BH_4)_2$·1.5-IPA (**s5***) from 1 Hz to 1×10^7 Hz at 28 to 40 °C is seen. At high frequencies the sample acts as a capacitor after which the phase drops to 10^3 Hz whereafter it increases to −70°. Above 5 MHz and below 10 Hz non-linear behaviour is observed, which is a limitation of the setup. These data points are excluded from analysis. In a pure ionic conductor with blocking electrodes (in this case molybdenum) the electrode/solid electrolyte interface acts as a capacitor, due to the charge build-up on each electrode being compensated by the electrode. This is modelled using Q_1 in the equivalent circuit. Furthermore, there will be a mass transfer resistance which is time dependent due to the change in local concentration of charges as diffusion through the electrolyte occurs. This along with the electrolyte resistance is combined in Q_2. R_1 represents the charge transfer resistance, which is the resistive characteristic of the interface.

In a situation where the distance between the electrodes is very small, a geometric capacitance will be present, and it is for our system as well. By compensating for the capacitance gained from the open circuit measurements, our peak frequencies will appear in the MHz range instead of the kHz range. This is done by measuring open and short circuit impedance of the cell and subtracting this contribution from the measured data. Furthermore, roughness at the electrode surface can cause the interphase to depart from ideal capacitance. However, this will not change the charge transfer resistance and will therefore not change the reported conductivities. The data corrected, based on the open and short circuit measurements, can be seen in Figure S2.

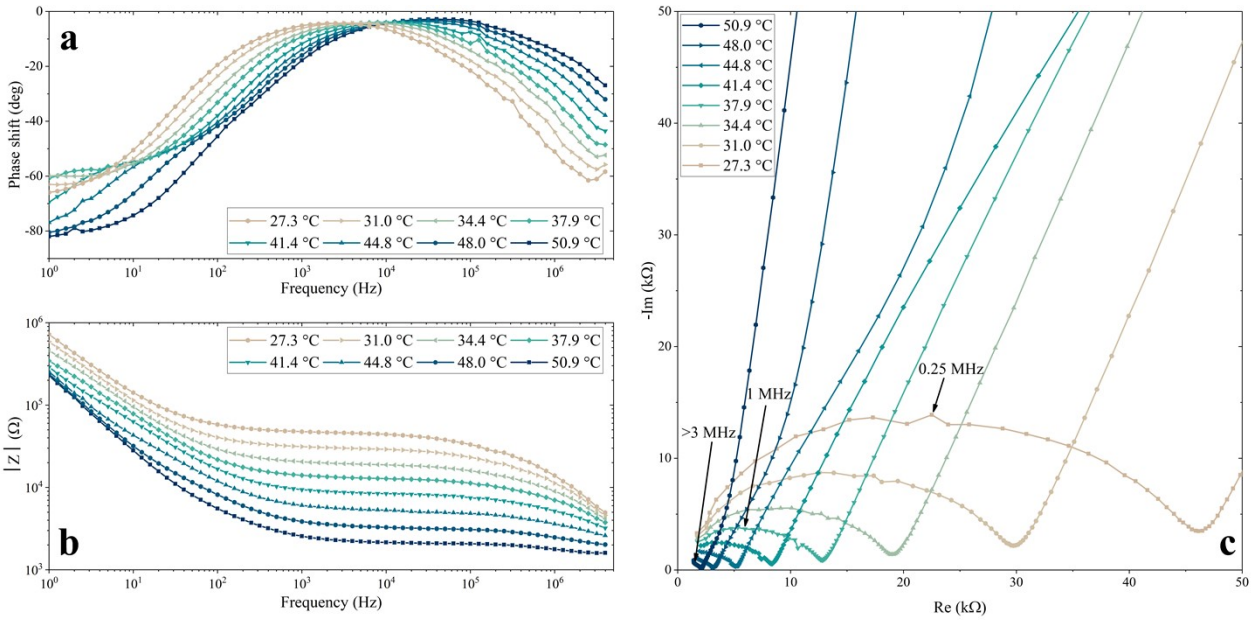

*Figure S2. Capacitance corrected Bode plot (a and b) and Nyquist plot (C) of $Mg(BH_4)_2$·1.5-IPA (**s5***) from 1 Hz to 5×10^6 Hz at 28 ℃ to 51 ℃. Compared to the uncorrected we see a similar resistance, however the peak frequencies are shifted up by a factor 10^3. Peak frequencies of data recorded at 27.3, 41.4 and 50.9 ℃ are marked in the figure.*

Cyclic Voltammetry (SI2)

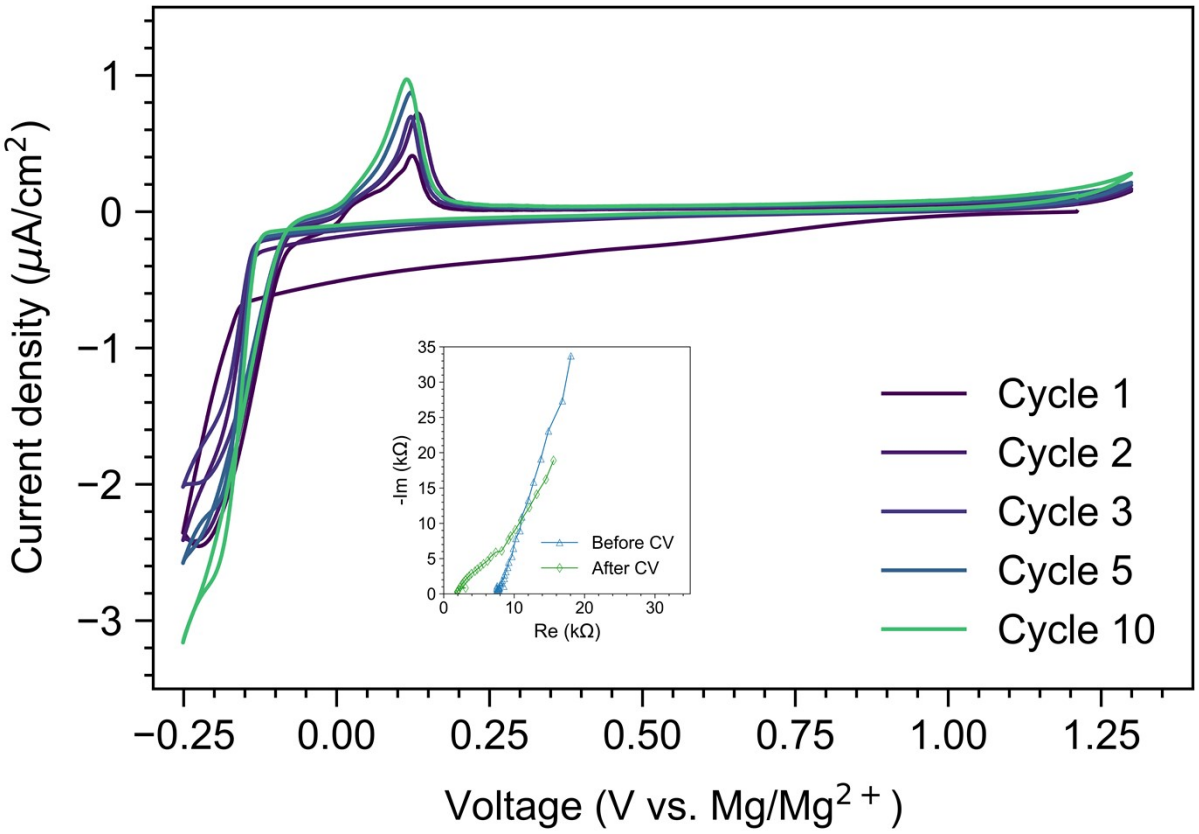

*Figure S3. Cyclic voltammetry of the $Mg(BH_4)_2 \cdot 1.5IPA$ (**s5***) at 40 °C, with molybdenum as the working electrode and magnesium as the counter/reference electrode in a two electrode setup, using a scan rate of 0.5 mV s^{-1}. Inset shows the Nyquist plot of EIS measurements before and after CV from 20 kHz to 10 Hz at 40 °C.*

Nuclear Magnetic Resonance (SI3)

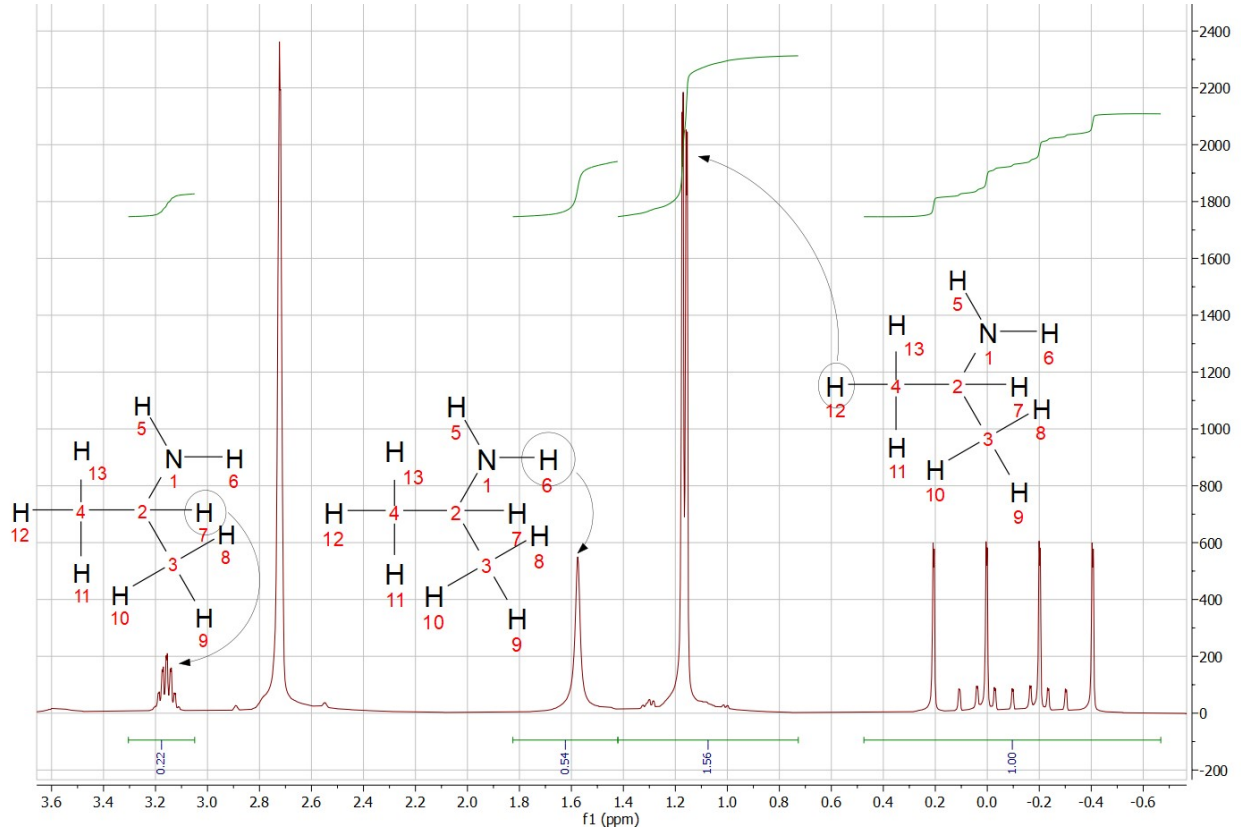

Figure S4. ***^{1}H Nuclear Magnetic Resonance:*** *NMR spectrum of $Mg(BH_4)_2{\cdot}2(CH_3)_2CHNH_2$* ***(s4)****. The large peak at 2.7 ppm is the solvent DMSO and the quartet at 0.4 to -0.6 is the BH_4^- group. This group is used as an integral reference as its amount is known.*

Table 1. ***^{1}H Nuclear Magnetic Resonance:*** *Signal integrals converted to sample composition in $Mg(BH_4)_2{\cdot}x$IPA using the known BH_4^- concentration as a reference.*

Sample	CH_3	CH	NH_2	x
s2	0.56	0.48	0.55	0.53 ± 0.05
s3	0.92	0.96	0.88	0.92 ± 0.04
s4	1.20	1.28	1.29	1.25 ± 0.06
s5	1.52	1.44	1.44	1.47 ± 0.04
s6	1.68	1.76	1.8	1.75 ± 0.07
s7	2.08	2.00	2.13	2.07 ± 0.07
s8	2.00	2.20	1.92	2.03 ± 0.17
s9	2.53	2.64	2.40	2.52 ± 0.12
s10	3.12	3.28	2.88	3.09 ± 0.21

^{1}H Nuclear Magnetic Resonance spectroscopy was performed on samples **s2** to **s10** to determine isopropylamine (IPA) coordination in the bulk samples. Using the signal from BH_4^- as a reference the coordination of isopropylamine can be found by the amount of characteristic hydrogen in the sample. Looking at the spectrum we identify the doublet at 1.15 ppm as the methyl groups. The integral of these peaks is 1.54, which is multiplied by eight as there are eight hydrogen atoms in the two BH_4^- reference groups. This number is then divided by the six hydrogen atoms per isopropylamine molecule giving an amount of IPA of 2.00. The singlet peak at 1.55 ppm is assigned to the NH_2^- group. Using the same method as the previous peak yields a coordination of 2.20. The signal at 2.7 ppm is assigned to the solvent DMSO.[1] The septet peak is assigned to the central C-H of the IPA molecule. The integral is corresponds to a coordination of 1.92. Averaging these values gives a coordination of 2.03 ± 0.17. A full spectrum can be seen in Figure S4.

Thermogravimetric Analysis, Differential Scanning Calorimetry and Mass Spectroscopy (SI4)

Figure S5 shows the simultaneous measurement of thermogravimetric analysis (TGA), differential scanning calorimetry (DSC) and mass spectrometry (MS) data of $Mg(BH_4)_2$·1.5-IPA (**s5**) (A) and $Mg(BH_4)_2$·1.5-IPA–MgO(75 wt%) (**s11**) (B). Due to the foaming nature of **s5**, a small amount of sample (1-2 mg) was used, and the individual data point is somewhat uncertain. At 53 °C we see a small release of IPA which might be an artifact as the same behaviour is observed for $Mg(BH_4)_2$·2IPA (**s7**) or a release of surface coordinated IPA. Between 85 and 122 °C a sharp increase in the release of IPA is observed, with a mass loss of 14 wt%. After this event a continuous release until 160 °C is observed where another faster mass loss is observed resulting in a total mass loss of 21 wt% between 160 and 209 °C. These releases are assigned to hydrogen release suggesting the sample decomposes during IPA release. Looking at Figure S5B (**s11**), we see no release of IPA at 53 °C and the first mass loss is at 132 °C. This is a significant shift of ~30 °C confirming that the addition of nanoparticles both mechanically and thermally stabilise the material. This is again observed for the second peak where the maxima were shifted 40 °C, however the mass loss occurs across a wider temperature range. A mass loss above 250 °C is observed for **s11** indicating a complete release of IPA. From 105 °C to 135 °C we see a mass loss of 2 wt% and MgO is inert in the entire temperature range this is an 8 wt% mass loss from $Mg(BH_4)_2$·1.5-IPA i.e. $Mg(BH_4)_2$·1.3-IPA. This compound has also been observed during prolonged drying of $Mg(BH_4)_2$·2-IPA. From 150 °C to 250 °C a mass loss of 11.5 wt% (46 wt% from $Mg(BH_4)_2$·1.5-IPA) accounting for the remaining 1.3-IPA indicating that only $Mg(BH_4)_2$ remains.

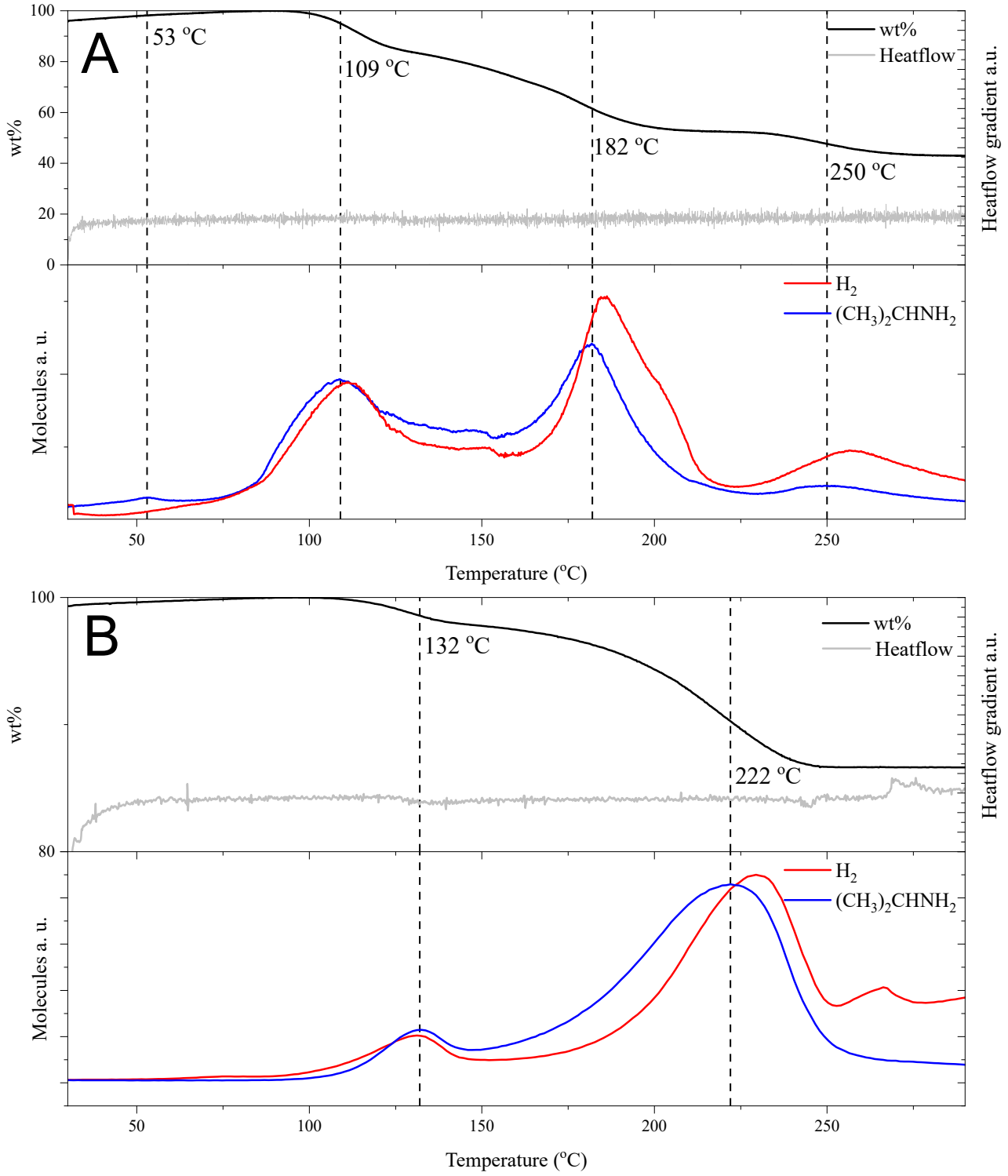

Figure S5. ***Thermogravimetric analysis, differential scanning calorimetry and mass spectrometry:*** *(A) (Top) Thermo gravimetric analysis and differential scanning calorimetry of $Mg(BH_4)_2$·1.5-IPA (**s5**). (Bottom) Mass spectrometry data the released gas from **s5** during thermogravimetric analysis. (B) (Top) Thermal gravimetric analysis and differential scanning calorimetry of $Mg(BH_4)_2$·1.5-IPA–MgO(75 wt%) (**s11**). (Bottom) Mass spectrometry of the released gas from **s11** during thermogravimetric analysis.*

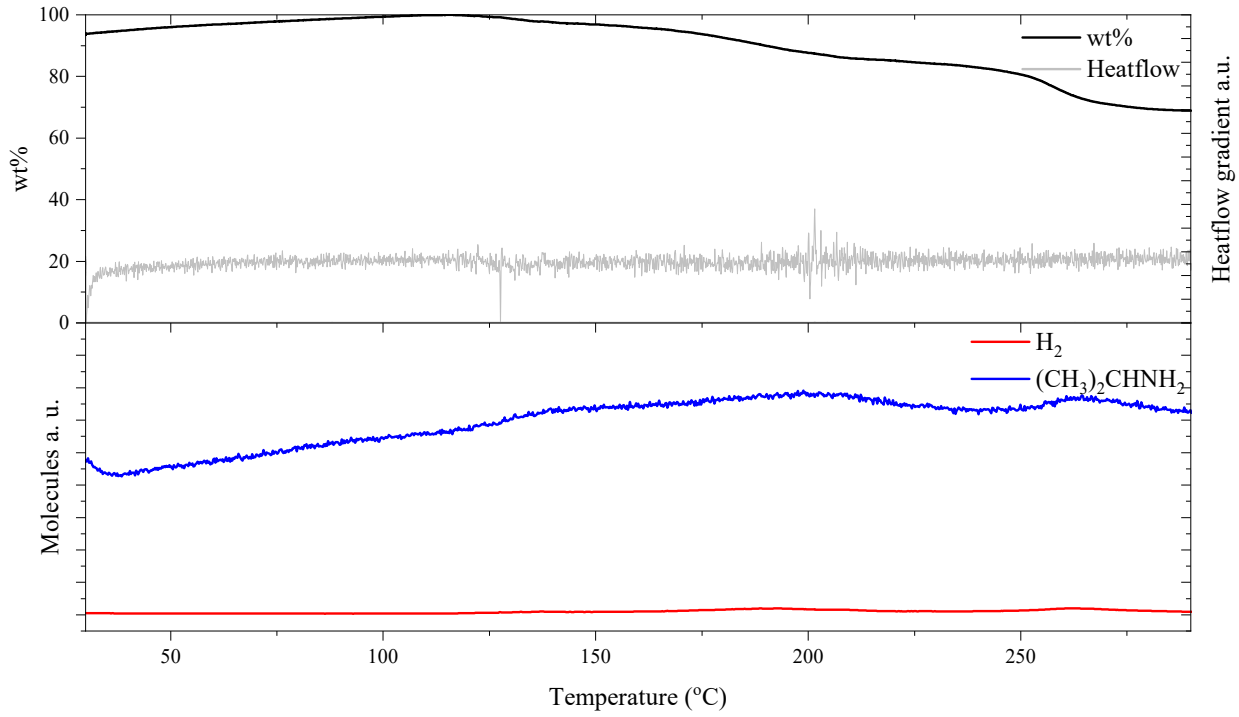

Figure S6 ***Thermal Gravimetric Analysis, Differential Scanning Calorimetry and Mass Spectrometry:*** *(Top)) Thermo gravimetric analysis and differential scanning calorimetry of $Mg(BH_4)_2$·0.5-IPA (**s2**). (Bottom) Mass spectrometry data the released gas from **s2** during thermogravimetric analysis.*

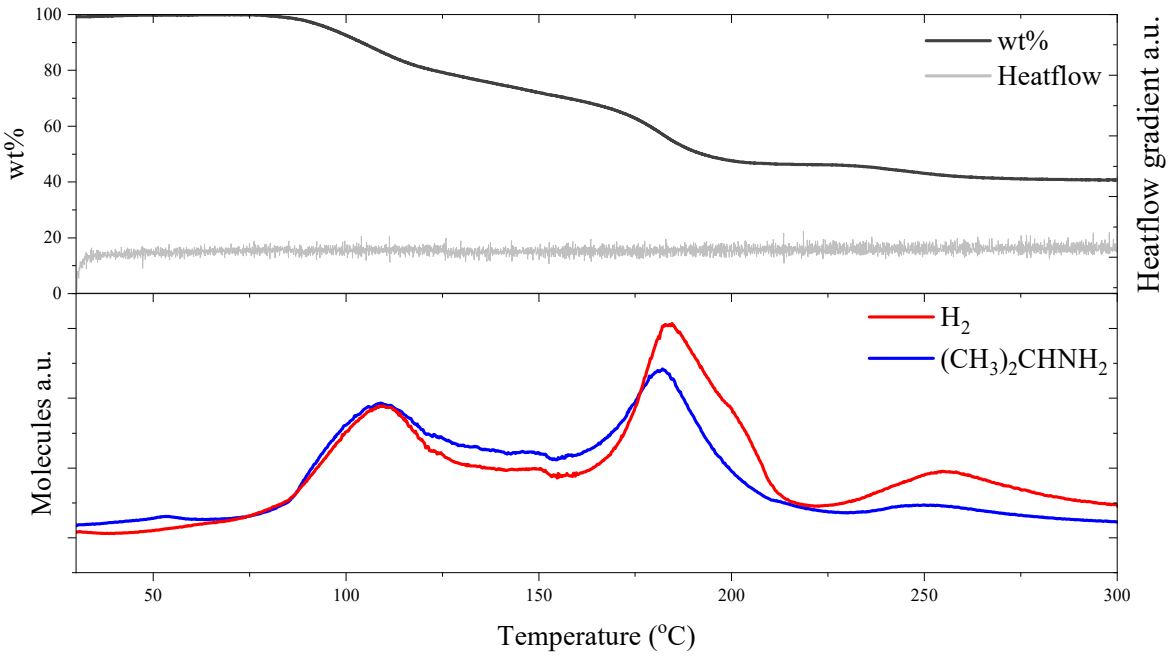

Figure S7 ***Thermal Gravimetric Analysis, Differential Scanning Calorimetry and Mass Spectrometry:*** *(Top)) Thermo gravimetric analysis and differential scanning calorimetry of $Mg(BH_4)_2$·2-IPA (**s7**). (Bottom) Mass spectrometry data the released gas from **s7** during thermogravimetric analysis.*

In situ synchrotron powder X-ray diffraction (SI5)

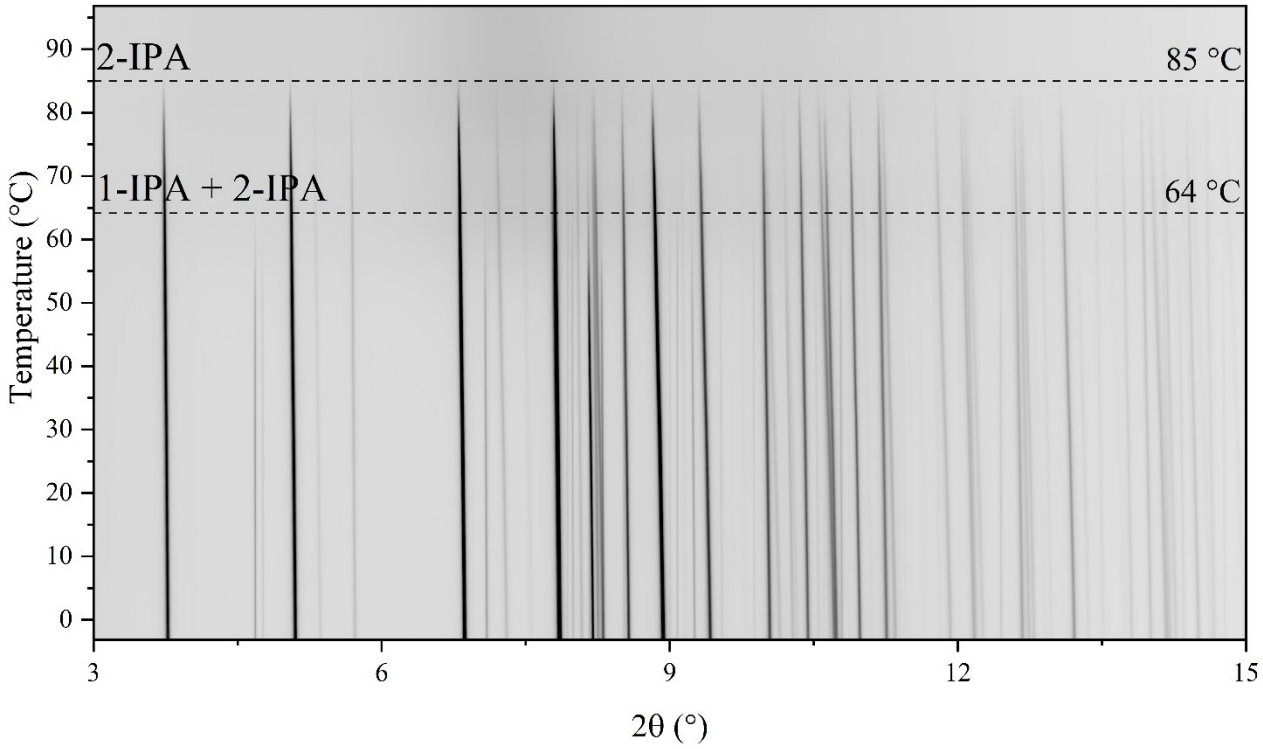

*Figure S8 In situ synchrotron X-ray powder diffraction data of $Mg(BH_4)_2 \cdot 1.75$-IPA (**s6**) from -3 °C to 97 °C. Here it is observed that the melting point of 1-IPA is significantly lowered compared what was observed in of $Mg(BH_4)_2 \cdot 0.9$-IPA **s3**. During melting of 1-IPA, the intensity of 2-IPA was also decreased. This suggests that eutectic melting occurs with an eutectic composition lower than 1.75-IPA.*

(1) Fulmer, G. R.; Miller, A. J. M.; Sherden, N. H.; Gottlieb, H. E.; Nudelman, A.; Stoltz, B. M.; Bercaw, J. E.; Goldberg, K. I. NMR Chemical Shifts of Trace Impurities: Common Laboratory Solvents, Organics, and Gases in Deuterated Solvents Relevant to the Organometallic Chemist. *Organometallics*, 2010, *29*, 2176–2179. https://doi.org/10.1021/om100106e.